A Novel Strategy for Radar Imaging Based on Compressive Sensing

Mariví Tello Alonso, *Student Member, IEEE*, Paco López-Dekker, *Member, IEEE*, and Jordi J. Mallorquí, *Member, IEEE*

***Abstract*—Radar data have already proven to be compressible with no significant losses for most of the applications in which it is used. In the framework of information theory, the compressibility of a signal implies that it can be decomposed onto a reduced set of basic elements. Since the same quantity of information is carried by the original signal and its decomposition, it can be deduced that a certain degree of redundancy exists in the explicit representation. According to the theory of compressive sensing (CS), due to this redundancy, it is possible to infer an accurate representation of an unknown compressible signal through a highly incomplete set of measurements. Based on this assumption, this paper proposes a novel method for the focusing of raw data in the framework of radar imaging. The technique presented is introduced as an alternative option to the traditional matched filtering, and it suggests that the new modes of acquisition of data are more efficient in orbital configurations. In this paper, this method is first tested on 1-D simulated signals, and results are discussed. An experiment with synthetic aperture radar (SAR) raw data is also described. Its purpose is to show the potential of CS applied to SAR systems. In particular, we show that an image can be reconstructed, without the loss of resolution, after dropping a large percentage of the received pulses, which would allow the implementation of wide-swath modes without reducing the azimuth resolution.**

***Index Terms*—Compressive sensing (CS), l_1 minimization, linear programming, matched filter, sparsity, synthetic aperture radar (SAR).**

I. Introduction

In TYPICAL imaging radars used in remote-sensing applications, the scene is observed by an antenna at different sensor positions. In the case of synthetic aperture radar (SAR) systems, the coherent information recorded at the different positions is used to synthesize a very long antenna to improve the azimuth resolution. The need to avoid azimuth ambiguities in the resulting radar image results in the requirement of a dense spatial sampling of the backscattered signal. This required dense sampling results in large data rates, which for orbital missions translate to large onboard memory and downlink throughput requirements. More fundamentally, for SAR systems, this dense sampling results in a minimum pulse repetition frequency (PRF) requirement, which fulfills the Nyquist sampling theory that in turn limits the maximum swath of the system. Due to the high amount of data generated, in cases where the downlink throughput is a constraint, data compression techniques are encouraged and often used [1]. For instance, the European Space Agency (ESA) distributes the raw data of the Envisat in a compressed format, resulting from an onboard signal data reduction algorithm [2].

Data compression relies on the principle that a useful signal is not perfectly chaotic. This implies that its samples are related by structural patterns, and as a consequence, there exists some degree of redundancy in the complete representation of the signal. By assuming that the signal is sparse in a certain basis, the new concept of compressed (or compressive) sensing (CS) states that it is possible to reconstruct a signal accurately from a highly incomplete number of samples, even with fewer measurements than what is considered to be necessary according to the Nyquist theory. Before the advent of the CS formalism over the past few years, different applications in very diverse areas have used ideas in this direction. This is the case, for example, of sparse arrays in imaging radars [3] or of the Microwave Interferometric Radiometer by Aperture Synthesis instrument used in the Soil Moisture and Ocean Salinity mission [4]. More recently, CS has already proven to have far reaching implications in a number of fields related to signal processing [5]: medical imaging [6], biosensing [7], geophysical data acquisition [8], hyperspectral imaging [9], communications [10], etc.

This paper proposes a novel method based on CS for the focusing of raw data in the framework of SAR. This technique is introduced as an alternative option to the traditional matched filtering, which can suggest new modes of operation or improve the performance of existing ones.

After reviewing the basic insights of CS theory (see Section II), the fundamentals of the alternative technique proposed will be presented, justified, and tested on 1-D simulated signals (see Section III). Then, the real SAR data from the European Remote Sensing (ERS) satellite will be used to validate the proposed method (see Section IV). The purpose of this test is to show the potential of CS applied to SAR systems. In particular, we show that an image can be reconstructed, with no loss of resolution, after dropping a large percentage of the received pulses. This would allow, for instance, the implementation of wide-swath modes with no reduction of the azimuth resolution.

Manuscript received July 21, 2009; revised January 8, 2010. Date of publication July 8, 2010; date of current version November 24, 2010. This work was supported by the Spanish Ministry of Science and Innovation and FEDER funds under Project TEC2008-06764-C02-01.

M. Tello Alonso is with the Remote Sensing Laboratory, Signal Theory and Communications Department, Universitat Politècnica de Catalunya, 08034 Barcelona, Spain, and also with the Institut Català de Ciències del Clima, Parc Científic de Barcelona, 08028 Barcelona, Spain.

P. López-Dekker was with the Remote Sensing Laboratory, Signal Theory and Communications Department, Universitat Politècnica de Catalunya, 08034 Barcelona, Spain. He is now with the Microwaves and Radar Institute, German Aerospace Center, Oberpfaffenhofen, 82234 Wessling, Germany.

J. J. Mallorquí is with the Remote Sensing Laboratory, Signal Theory and Communications Department, Universitat Politècnica de Catalunya, 08034 Barcelona, Spain (e-mail: mallorqui@tsc.upc.edu).

Color versions of one or more of the figures in this paper are available online at http://ieeexplore.ieee.org.

Digital Object Identifier 10.1109/TGRS.2010.2051231

II. Theory of CS

This section exposes briefly the theoretical fundamentals of CS, introduced in [23] and [24]. A detailed presentation can be found in [5].

Consider a finite signal $x \in \mathbb{R}^N$ and a limited number of observations of x in the form of K linear measurements y_k

$$y_k = \langle x, \psi_k \rangle, \qquad k = 1, \ldots, K \tag{1}$$

where $\langle \ldots \rangle$ means the scalar product and ψ_k is known as the test signal. Therefore, the coefficients y_k result from the projection of the signal x on a set of fixed vectors. Equivalently, in matrix notation

$$y = \Phi x \tag{2}$$

where test vectors ψ_k constitute the rows of matrix Φ and the vector y is formed by the K elements y_k in (1). If there are much more unknowns than observations, $K \ll N$, (matrix Φ has much more columns than rows), the system of equations in (2) is highly undetermined. It has been shown in the framework of CS theory that it is very likely to recover x exactly provided that it is sparse and that matrix Φ obeys a restricted isometry condition (RIC). The recovery is achieved by means of an estimation through a convex optimization problem, designed as (P1) and described as

$$(\text{P1}) \min_{\tilde{x} \in \mathbb{R}^N} \|\tilde{x}\|_{l_1} \text{ subject to } y = \Phi \tilde{x}. \tag{3}$$

The linear program in (3) states that among all the signals $\tilde{x} \in \mathbb{R}^N$ that satisfy $y = \Phi \tilde{x}$ (this means that they all have the same representation in the projection on the set of K vectors ψ_k), we take the one that minimizes the l_1 norm given by

$$\|\tilde{x}\|_{l_1} := \sum_{k=1}^{N} |\tilde{x}_k|. \tag{4}$$

The l_1 norm is directly the sum of the absolute values of all the samples $\tilde{x}_k$ of vector $\tilde{x}$. By imposing the minimization of this norm, we are considering that the signal that we are looking for is the sparsest one among all the signals sharing an identical projection of the set of elements ψ_k [28].

It should be mentioned that the solution to the linear program in (3) does not require any particular *a priori* assumption about the number of nonzero elements in x nor about their locations and amplitudes. The literature provides several options of algorithms to solve (3). The most relevant ones are the basis pursuit (BP) [11], the matching pursuit (MP) [12], and the orthogonal matching pursuit (OMP) [13] techniques.

Let us consider more closely the requirements previously mentioned—the sparsity of x and the RIC of matrix Φ. On the one hand, according to sparsity, a signal x is sparse if there exists a domain ψ in which the coefficient sequence is supported on a small set. This means that significant information is carried by just a few coefficients. On the other hand, the RIC was first introduced by Candes and Tao [24]. It is related to the incoherency of the sets of columns of the matrix. In the scope of this paper, it will be used so that a sufficient condition for matrix Φ fulfills the RIC with a high probability and that its columns approximately behave like an orthogonal system.

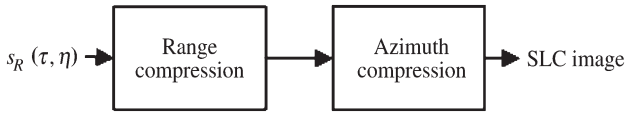

Fig. 1. Simplified SAR focusing by means of sequential compression in range and in azimuth.

Moreover, it has been shown [14] that the rationale exposed in this section can be extended to compressible noisy complex signals. It is worth noting that compressibility is a condition far less restrictive than sparsity, and most of the natural and manmade signals satisfy it. Compressibility implies that there exists a basis, in which the projection of the compressible signal produces just a small amount of coefficients with high energy. Similarly, linking the concepts of compressibility and sparsity, a signal is compressible if there exists a basis in which its projection is sparse.

III. Novel Radar Imaging Technique

This section presents a new method for focusing raw data in the framework of radar imaging after reviewing the operation and main drawbacks of the traditional matched-filtering approach.

A. Conventional Focusing Through Matched Filtering

In conventional imaging radar systems, the received signal is usually processed with a matched filter. This operation essentially consists in convoluting the received signal with a suitable reference function.

For SAR systems, this matched-filtering operation is applied in two steps [15, Ch. 2]: range compression and azimuth compression. In Fig. 1 s_R is the received signal, h_r is the impulse response of the filter in the range, h_a is the impulse response of the filter in the azimuth, and τ and η are the range (fast time) and azimuth (slow time) coordinates, respectively.

Matched filtering maximizes the signal-to-noise ratio (SNR) if additive white noise is assumed, and it is, therefore, the optimum solution in terms of the SNR. However, matched filtering typically results in relatively high sidelobes, which are usually mitigated by windowing the reference signal. With this tapering, the sidelobes are reduced, as well as the resolution.

From an implementation point of view, matched filtering assumes that the sampling frequency and the PRF satisfy the Nyquist–Shannon criterion. In the range, this can become a technological challenge if very high resolution is required. In the azimuth, however, it introduces fundamental tradeoffs between swath width, range ambiguities, and azimuth resolution [16, Ch. 2].

The next section exposes an alternative option to matched filtering.

B. CS Applied to Radar Imaging: State of the Art

In the last two years, several works have been proposed in the direction of radar imaging involving CS tools. The most relevant are mentioned hereafter.

In [25], the authors propose a new "compressive radar receiver," based on the notion of CS. They propose lowering the rate of the A/D converter in the receiver, projecting the resulting signal in a particular sparsity frame, and then inferring the observed signal by means of OMP greedy algorithms. They present the preliminary results of the simulated SAR imagery, with no speckle and regular shapes well adapted to the nature of the sparsity frame employed. In [26], sparse signal representation and approximations from complete dictionaries are explored. An application for the interpretation of airborne SAR wide-angle images is proposed. It suggests moving from a pixel representation to an object-level representation. No results with real data are provided. In [27], an alternative technique for the compression of raw data is proposed based on the use of dual-tree continuous wavelet transform as a sparsifying transform previous to the application of OMP in order to obtain a sparse representation of the complex SAR image.

C. Theoretical Principles of the Novel Approach for Radar Imaging Based on CS

Under the Born hypothesis [17]–[19], it can be assumed that the signal returned to the sensor $s_R(t)$ can be modeled as the convolution of the transmitted signal $s_T(t)$ with the reflectivity of the observed scene $\sigma(t)$

$$s_R(t) = s_T(t) \cdot \sigma(t) = \int_{-\infty}^{\infty} s_T(t-t')\sigma(t')dt'. \tag{5}$$

In practice, the received signal $s_R(t)$ is digitized with a sampling rate $1/k_1$. Variable t' in the integral in (5) is a dummy variable which can be discretized in the most general case with a different sampling rate $1/k_2$; the continuous case corresponds to infinitely short intervals k_2. Thus, $t = k_1 n$ and $t' = k_2 m$, where m and n are the discrete time variables corresponding to t and t', respectively, in the continuous domain. The convolution in the discrete domain can then be expressed as

$$s_R(k_1 n) = \sum_m s_T(k_1 n - k_2 m)\sigma(k_2 m). \tag{6}$$

If dealing with finite-length signals (the swath width τ_p is not infinite), the convolution can be expressed as a product of a matrix S with a vector σ. Let us consider for notation simplification purposes that $k_1 n = k$ and $k_2 m = j$ and that the signals considered have samples ranged from 1 to N, where N is the signal length. We assume the same length for s_T and σ, for the sake of simplicity. Then, the discrete convolution can be expressed as

$$s_R = S \cdot \sigma \begin{bmatrix} s_R(1) \\ s_R(2) \\ \vdots \\ s_R(N) \\ s_R(N+1) \\ \vdots \\ s_R(2N-2) \\ s_R(2N-1) \end{bmatrix} = \begin{bmatrix} s_T(1) & 0 & \cdots & 0 \\ s_T(2) & s_T(1) & \cdots & 0 \\ \vdots & \vdots & \ddots & \vdots \\ s_T(N) & s_T(N-1) & \cdots & s_T(1) \\ 0 & s_T(N) & \cdots & s_T(2) \\ \vdots & \vdots & \ddots & \vdots \\ 0 & 0 & \cdots & s_T(N-1) \\ 0 & 0 & \cdots & s_T(N) \end{bmatrix} \begin{bmatrix} \sigma(1) \\ \sigma(2) \\ \vdots \\ \sigma(N-1) \\ \sigma(N) \end{bmatrix}. \tag{7}$$

Matrix S is the convolution matrix, whose rows are reversed, conjugated, and time-shifted versions of the samples of $s_T(t)$. Vector σ is the sampled version of the reflectivity of the observed scene, and $s_R(n)$ is the sample acquired by the receiver. Hence, $s_R(n)$ can be considered as the result of the projection of the reflectivity of the observed scene $\sigma(n)$ onto the basis of the vectors constituting the rows of matrix S. At this point, the goal is to infer, as closely as possible, $\sigma(n)$ from the samples $s_R(n)$. It can be seen in Section III-A that, traditionally, σ is estimated by convoluting $s_R(n)$ with the corresponding matched filter of $s_T(t)$. We propose instead a recovery scheme based on CS.

In order to bring (7) to a CS scheme, there exist several options, depending if we consider similar or different sampling rates $1/k_1$ and $1/k_2$. Note, for example, that if we set the value of the blind variable k_2 to a value lower than k_1 (this is feasible since the analytical expression of the transmitted waveform is known *a priori*), the linear system in (7) is directly undetermined. Nevertheless, for the sake of clarity in the exposition, only one of the possible options is explored in detail in this paper. Essentially, this option considers $k_1 = k_2$, and it consists in reducing the amount of samples collected in the receiver. By doing so, in the formulation of the system of linear equations in (7), a reduced set of samples selected randomly is used in (8), leading to an undetermined system of equations

$$s'_R = S' \cdot \sigma' \begin{bmatrix} s_R(1) \\ \cancel{s_R(2)} \\ \vdots \\ \cancel{s_R(N)} \\ s_R(N+1) \\ \vdots \\ \cancel{s_R(2N-2)} \\ s_R(2N-1) \end{bmatrix} = \begin{bmatrix} s_T(1) & 0 & \cdots & 0 \\ \cancel{s_T(2)} & \cancel{s_T(1)} & \cdots & \cancel{0} \\ \vdots & \vdots & \ddots & \vdots \\ \cancel{s_T(N)} & \cancel{s_T(N-1)} & \cdots & \cancel{s_T(1)} \\ 0 & s_T(N) & \cdots & s_T(2) \\ \vdots & \vdots & \ddots & \vdots \\ \cancel{0} & \cancel{0} & \cdots & \cancel{s_T(N-1)} \\ 0 & 0 & \cdots & s_T(N) \end{bmatrix} \times \begin{bmatrix} \sigma(1) \\ \sigma(2) \\ \vdots \\ \sigma(N-1) \\ \sigma(N) \end{bmatrix}. \tag{8}$$

In (8), the neglected samples appear crossed out. They will not be taken into account for the retrieval of vector σ. In such a situation, x can be retrieved exactly with a number of measurements on the order of $\alpha \log(N)$, where α is the order of sparsity of x. Note that a signal α sparse means that it has only α nonzero coefficients in a suitable transformed domain.

From a computational point of view, the solution of the CS scheme is more time consuming than the convolution with the matched filter. The convex program, expressed in (3), has a computational load of about 30 or 50 times that of solving a least-square problem of equivalent dimensions [20]. In Section II, different options have been mentioned to deal with this matter. In the framework of this paper, we choose the use of a regularized OMP (ROMP), since it provides an efficient and robust solution and is able to handle complex noisy data [13].

The ROMP is an iterative algorithm performing a local optimization as opposed to the global optimization techniques, such as the BP, for example. Essentially, at each iteration, the MP looks for the element of the basis ψ_k which is the most strongly correlated with the signal x, that is, which has the highest absolute inner product with the signal. The estimated signal is then actualized accordingly.

D. Fulfillment of the Requirements to Apply CS

The theory of CS states two requirements (see Section II) in order to expect a valid solution to the highly undetermined system in (8). This section shows that it is reasonable to employ CS for radar imaging purposes, since both conditions are fulfilled.

1) Sparsity of Radar Data: It is widely assumed that compressibility is expected for signals whose power spectrum drops with increasing frequency, i.e., they belong to the $1/f$ family. The amplitude of a SAR image follows a characteristic gamma distribution, and thus, its spectrum drops with frequency even if not as fast as that for an optical image [15, Ch. 4]. Moreover, the sparsity (in a wider sense, the compressibility) of radar data has been already justified in the literature, and different image-coding algorithms have been proposed for radar data compression, based on this condition [1], [21].

2) Convolution Matrix Satisfies RIC: The RIC says that the mapping Φ acts like an isometry on α-sparse vectors. It requires that every set of columns with a cardinality less than α approximately behaves like an orthonormal system. That is to say all subsets of α columns taken from Φ are nearly orthogonal. By construction, the convolution matrix is a band matrix. The real part of a convolution matrix used in the 1-D simulations of Section III-D is shown in Fig. 2 (left). The green color corresponds to zeros, and as a consequence, it can be observed that nonzero elements are distributed following a band crossing the matrix from the upper left corner to the bottom right one. In a band matrix, the scalar product between two nonconsecutive columns involves a small number of nonzero coefficients (decreasing when the distance between the columns augments). Since matrix Φ is directly obtained from the convolution matrix, after the removal of a number of rows (see Fig. 2, on the right), the observations according to the orthogonality of columns raised for the convolution matrix still hold for matrix Φ. Thus, the orthogonality is just to be verified between columns close to each other.

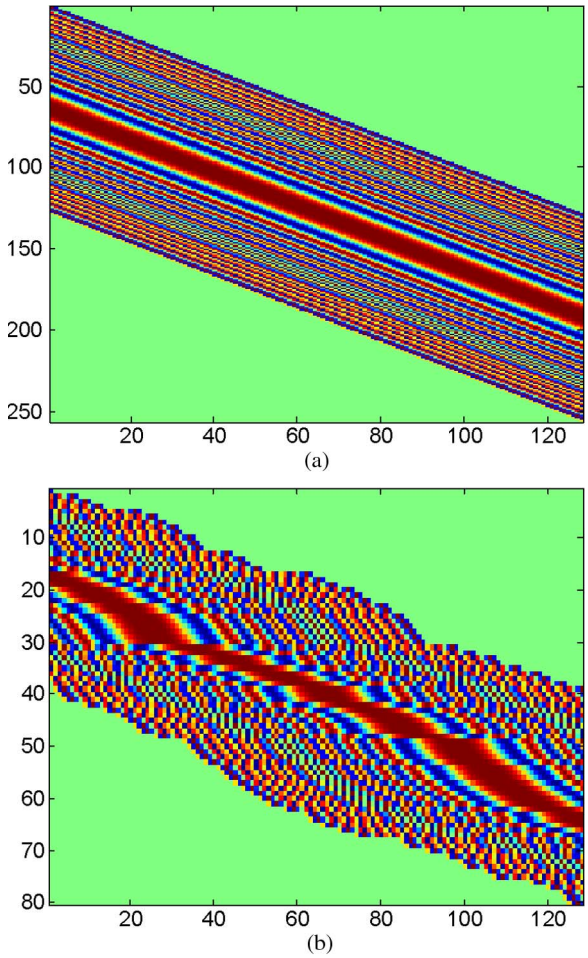

Fig. 2. Representation of both the convolution matrix (a) and matrix Φ obtained after random selection of rows (b).

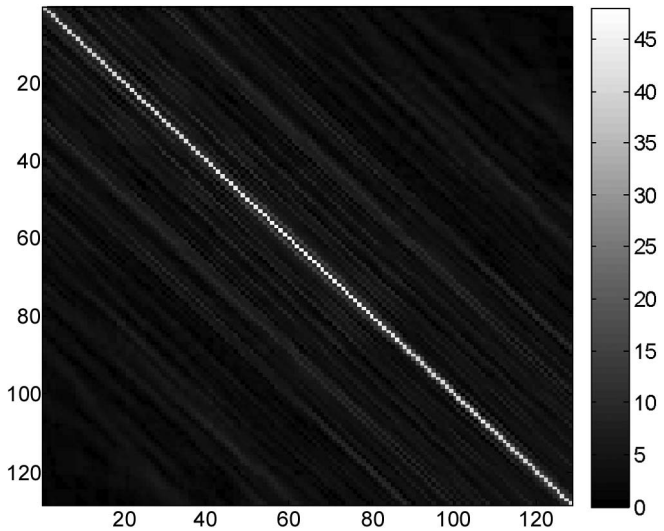

Fig. 3. Representation of the autocorrelation matrix of the columns of matrix Φ in Fig. 2.

In this sense, it is easy to verify that the orthogonality between two consecutive columns in a band matrix depends directly on the autocorrelation of the samples constituting these

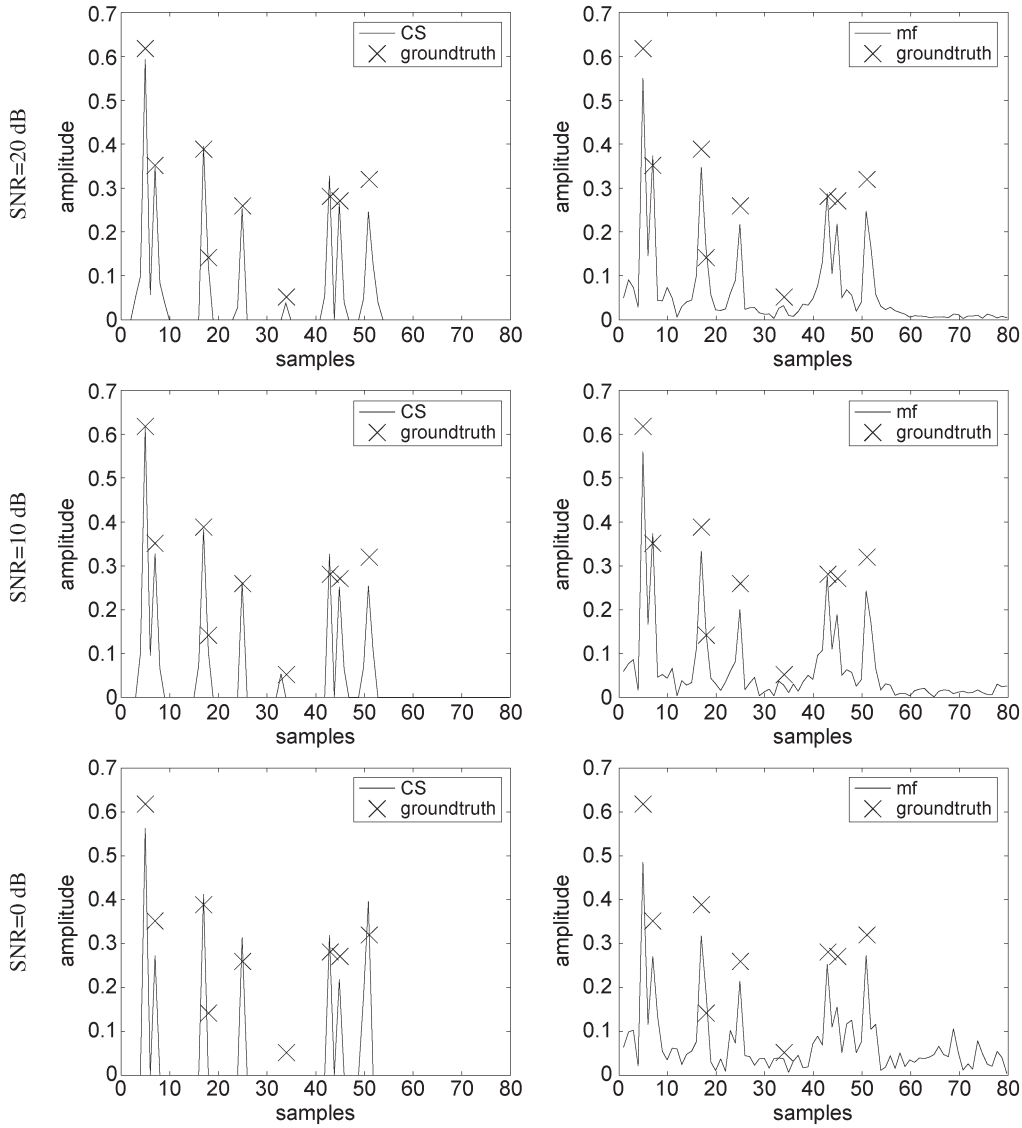

Fig. 4. Amplitude retrieved for a simulated scene with ten point targets with different SNR levels, ranging from 0 to 20 dB. (Left column) Results obtained with the technique based on CS, with 50% of the samples (solid curve) superimposed to ground truth (x mark). (Right column) Results obtained with matched filtering (solid curve) superimposed to ground truth (x mark).

columns. In the particular case that we are considering, the column vectors are the samples of the transmitted waveform which consists in a chirp signal. Since the autocorrelation of a chirp signal is low except at the origin, the orthogonality of the columns of matrix Φ is verified. Fig. 3 represents the autocorrelation matrix of the columns of matrix Φ in Fig. 2. It can be observed that this matrix is almost the identity, and as a consequence, it is verified that Φ satisfies the RIC.

E. One-Dimensional Simulation Results

In order to check the viability of the alternative radar imaging technique exposed in this paper, the first test has been carried out on a set of simulated 1-D signals.

The procedure of the simulation is enumerated in the following sentences. First, the round-trip delay for a collection of point targets is randomly generated using a uniform distribution corresponding to a range of valid distances. Then, the complex scattering coefficient of each target is randomly chosen from a Rayleigh distribution in amplitude and a uniform distribution in phase. Finally, the received signal is generated as the sum of the time-shifted replicas of the transmitted waveform (which is adjusted to be a chirp signal with a compression ratio of 52); each is multiplied by its respective scattering coefficient. Once the received signal has been synthesized, a random white Gaussian noise vector is added to simulate the thermal noise.

In reception, in order to build a CS scheme as in (2), the first step is to construct the convolution matrix Φ from the known transmitted waveform. Then, just a fraction of the samples of the simulated received signal have been kept (see Fig. 2). These samples are taken randomly. In the framework of this paper, the experiments have been carried out with 10% to 70% of the samples. Hence, a reduced convolution matrix results from this selection with the rows of matrix Φ corresponding to the samples selected. It has been empirically observed that

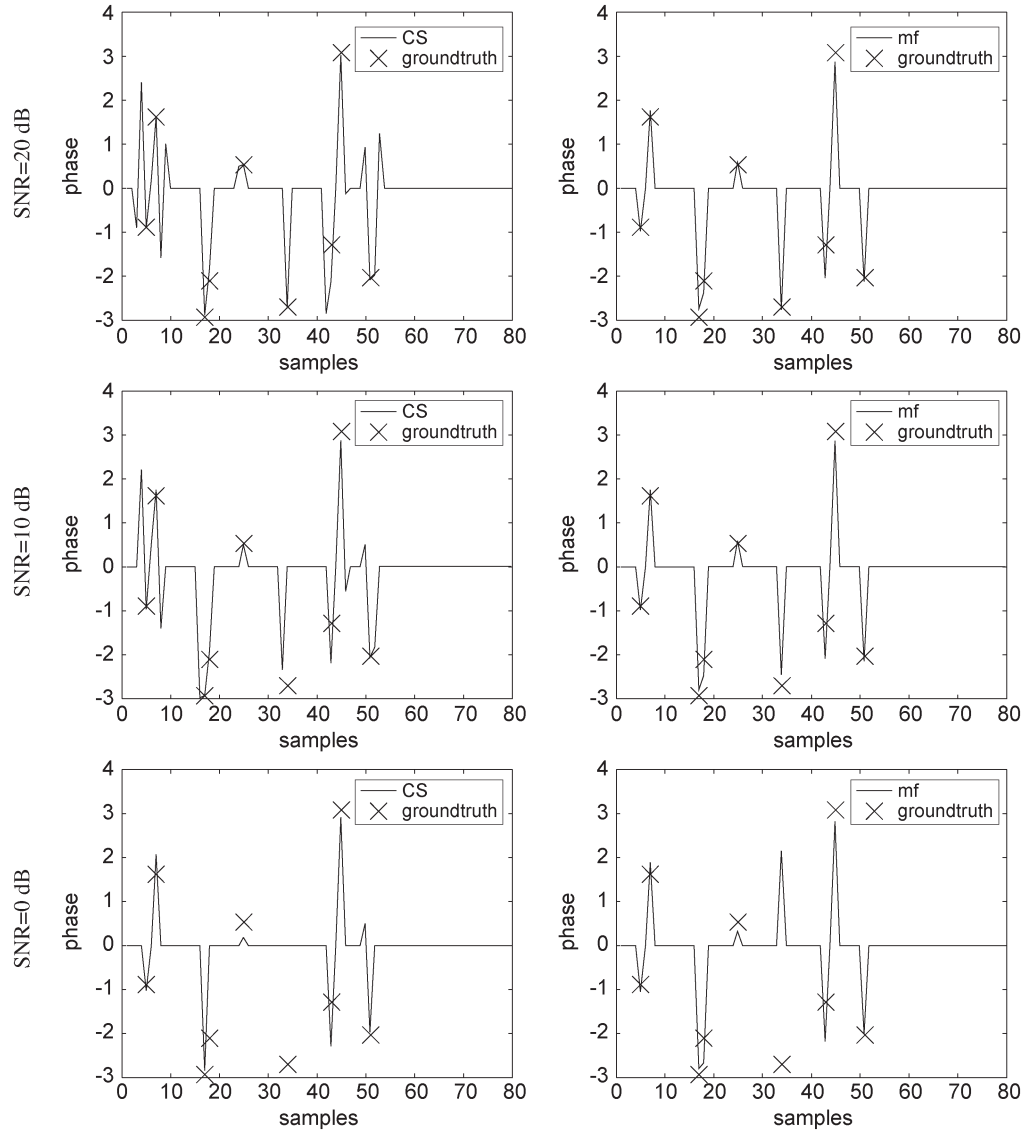

Fig. 5. Phase retrieved for the same simulated scene in Fig. 4, with ten point targets with different SNR levels, ranging from 0 to 20 dB. (Left column) Results obtained with the technique based on CS, with 50% of the samples (solid curve) superimposed to ground truth (x mark). (Right column) Results obtained with matched filtering (solid curve) superimposed to ground truth (x mark).

a higher number of samples slightly reduce the error of the estimated signal. Nonetheless, the results shown in this paper have been obtained by setting the number of samples considered for the estimation to 50% of the samples received. Once the undetermined system of equations is constructed, the convex linear problem in (3) is solved with the ROMP algorithm. In order to evaluate the possibilities of this new radar imaging technique with respect to the traditional ones, results have been compared with those of the matched filtering. Figs. 4 and 5 show, respectively, the amplitude and the phase obtained by the method based on CS (left column), as well as with matched filtering (right column), for an example of simulated scene with ten point targets. In order to test and compare the robustness in front of noise of both methods, tests were carried out with no noise, as well as with SNRs ranging from -10 to 20 dB.

The results are summarized by representing only three cases (0, 10, and 20 dB). The selection of this range of values obeys to the fact that most of the changes were observed in this region. The results are superimposed to the ground truth (represented by x marks) in order to highlight the mismatches. Moreover, it is worth noting that for the phase resulting from matched filtering, only the points with a target in the ground truth have been considered, since the phase can be seen as noise elsewhere.

On the one hand, according to the amplitude, for SNRs greater than 10 dB, the method based on CS exhibits a close match to the ground truth: The targets are detected with accurate amplitudes at the right positions, and no artifacts appear. The most noticeable effect compared to matched filtering is the complete absence of sidelobes. This permits a better discrimination of close targets (see targets located between positions five and ten), as well as the avoidance of a ringing effect for low SNRs (see target at position 25 for an SNR equal to 0 dB). Moreover, sidelobes produced by matched filtering can also hide low-amplitude targets. For instance, it can be observed that the low-amplitude target located near position 35 is detected with the technique proposed based on CS for SNRs greater

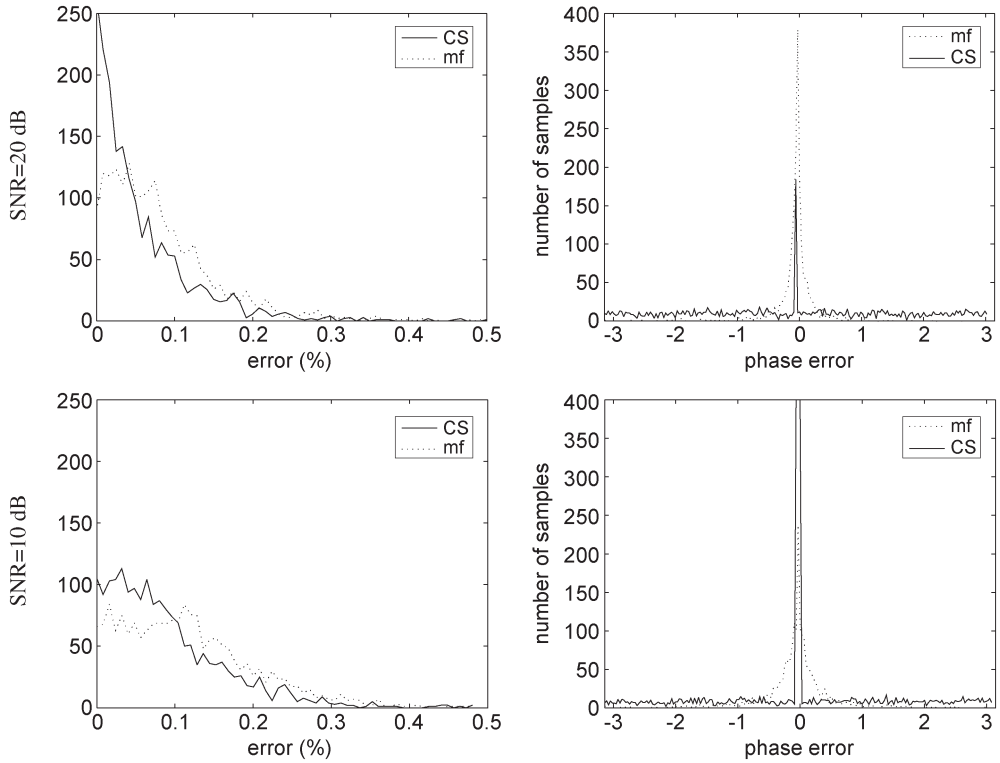

Fig. 6. Histograms of the errors produced by the CS approach (solid curves) and by matched filtering (point curves) for both amplitude (left column) and phase (right column) and for different SNRs.

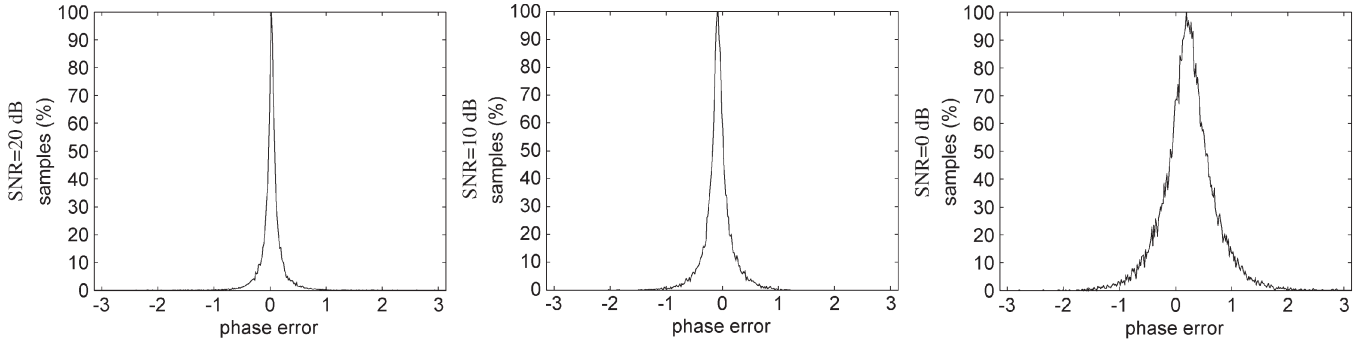

Fig. 7. Histograms of the phase difference introduced by the CS approach for different realizations.

than 0 dB, while it does not appear in the result obtained with matched filtering for any SNR. On the other hand, according to the phase plots, a more precise match to the ground truth is observed for the values retrieved with the technique based on CS than for those obtained through matched filtering (the comparison is considered only for nonzero elements). However, even for high SNRs, artifacts are introduced. Moreover, as observed for the amplitude, for an SNR lower than or equal to 0 dB, the method is unable to detect the lowest amplitude target in the example of the simulation selected. In order to evaluate and compare the errors introduced in the recovery by means of the technique proposed based on CS, as well as with the traditional matched filter, a systematic test has been carried out over 200 different simulated scenes. For each one, the relative errors in amplitude and in phase have been evaluated separately. The phase error has been estimated as the phase of the product of the result with the complex conjugate ground-truth signal. For the phase of the result obtained through matched filtering, only the points corresponding to the presence of targets have been considered. The histograms of the errors, both in amplitude and in phase, for the processing with CS (red curves), as well as with the conventional matched filtering (blue curves), are represented in Fig. 6. It can be observed that the histograms corresponding to the error introduced by the CS approach exhibit important peaks at zero and low values elsewhere, both in amplitude and in phase.

Since the selection of the 50% of the samples intervening in the CS approach is done randomly, the repeatability of the method proposed has to be checked. In order to do so, the phase difference between the results obtained with 20 realizations for each of 200 simulated examples has been computed. Additionally, the test has been extended to different SNRs. The results are shown in Fig. 7 in which it can be observed the rapid decay of the dispersion of phase differences as a function of the amplitude in any case. As the SNR decreases, the values tend to show a larger spread.

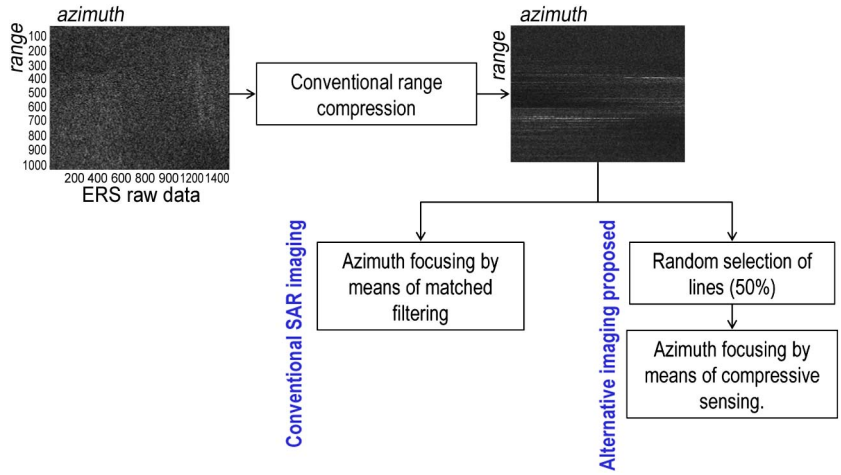

Fig. 8. Flowchart of the experiment carried out with SAR raw data.

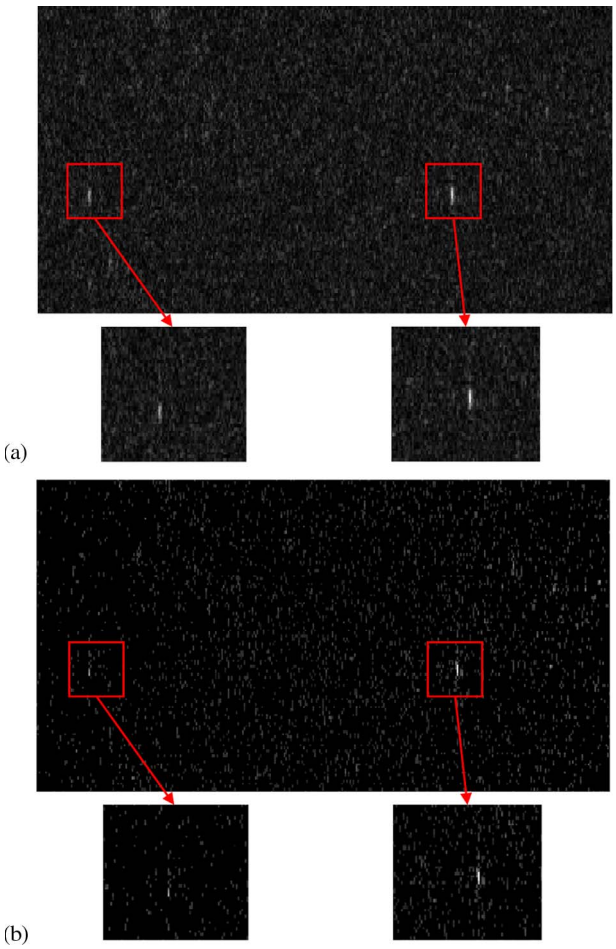

Fig. 9. Example of test of the proposed technique based on CS on an oceanic scene. (a) Single-look complex image obtained by means of conventional SAR imaging. (b) Single-look complex image obtained by means of CS imaging, with 50% of the lines.

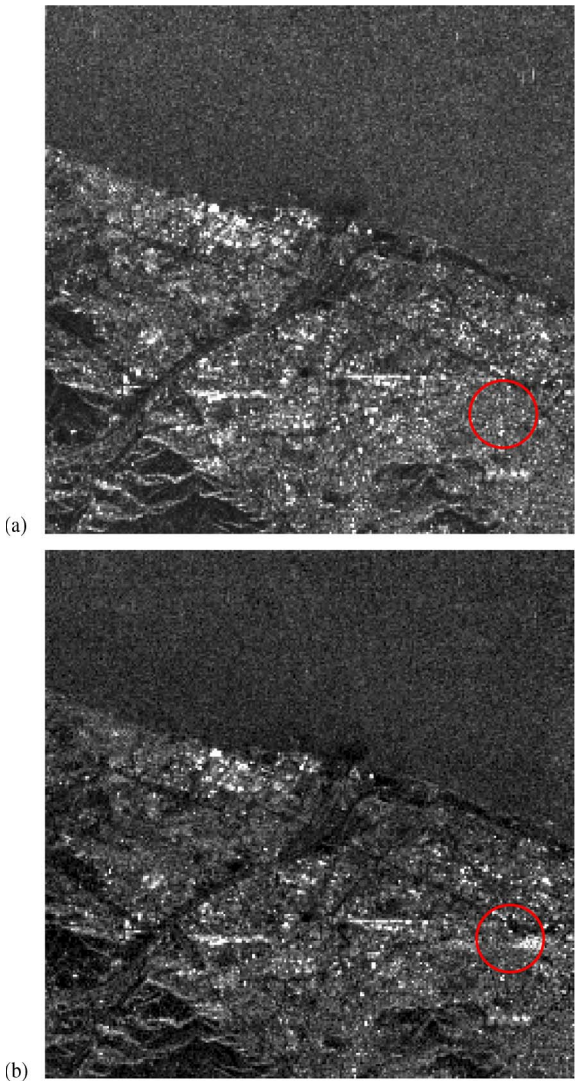

Fig. 10. Example of test of the proposed technique based on CS on a complex scene. (a) Multilooked image obtained by means of conventional SAR imaging. (b) Multilooked image obtained by means of CS imaging, with 50% of the lines.

IV. Results With SAR Data

After confirming the viability of the proposed approach through testing on sparse 1-D simulated data, an application has been explored in the framework of SAR processing. It considers

an alternative method for the compression of raw data, and it has been carried out with data acquired with the ERS-2 sensor of the ESA of the area in the city of Barcelona, Spain, on October 10, 1999. The results presented in this section are the preliminary ones. They constitute the first experiments of the azimuth compression involving real data. However, since SAR data are not sparse in practice, the quality of the results is not optimum, and it would be improved by adding a projection in a sparsifying matrix in the reception.

A. Description of the Processing

Section III-A has already provided a brief overview of the conventional process of SAR focusing. With more detail, according to a range Doppler algorithm (RDA) without range cell migration correction, the compression of raw data is done in two steps: range and azimuth compression. Assuming the separability of processing in these two directions, the operations are performed sequentially with 1-D arrays.

In the scope of this experiment, the procedure applied consists in processing the data in the range direction by means of conventional compression with matched filtering and then focusing in the azimuth with the technique proposed based on CS (see Fig. 6). Specifically, let $S_R(f_\tau, \eta)$ be the range Fourier transform of $s_R(\tau, \eta)$, the demodulated radar signal. Let $H_R(f_\tau)$ be the frequency domain matched filter in the range. The output of the range compression can be expressed as [22]

$$s_{RC}(\tau, \eta) = IFFT_\tau \left\{ S_R(f_\tau, \eta) H_R(f_\tau) \right\}. \tag{9}$$

Once the compression in the range is completed, for each sample vector in the range, instead of applying matched filtering in the azimuth, we consider a random selection of 50% of the lines in the azimuth. These lines constitute a vector s_R in (7), and hence, the rows of the convolution matrix Φ (built as previously through the *a priori* known expression of the transmitted waveform) are selected accordingly. Then, once the elements of the linear program in (3) are identified, we use the ROMP algorithm to solve it, just as in the case of the tests with the simulated examples in Section III-D.

A rigorous quantitative evaluation of the effects of the technique proposed based on CS is difficult to provide since, in real scenarios, no precise ground truth is available. As a consequence, only a qualitative estimation is provided, taking the traditional focusing with matched filtering as a reference (see Fig. 8).

B. Results

This section provides an overview of some illustrative results obtained.

The first set of tests has been carried out in oceanic scenes. If assuming applications exclusively concerned by the presence and position of ships, sea clutter can be treated as noise. As a consequence, this produces an extremely sparse signal well suited for the application of CS techniques. An example with two vessels is shown in Fig. 9. Both targets are detected with sufficient contrast with respect to the background, and they are located at the correct positions. Furthermore, it must be noted that they appear with an azimuth smearing less accentuated than with that of the processing with conventional focusing. However, it must be noted that the presence of the target in the left is less noticeable in the retrieval by means of CS than in the one with the conventional matched filter. Because of the nonavailability of the ground truth, the interpretation of this observation is delicate. It could be due to the simplistic assumption of the sparsity of SAR data, but it could also be due to the nature of the target.

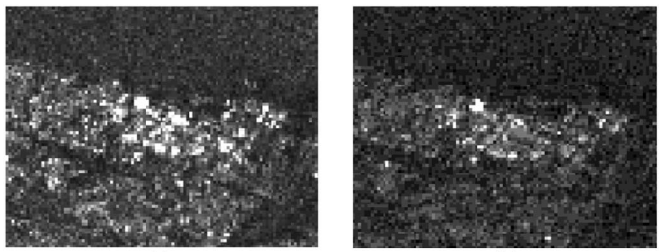

(a) (b)

Fig. 11. Zoom on a urban area. (a) Multilooked image obtained by means of conventional SAR imaging. (b) Multilooked image obtained by means of CS imaging, with 50% of the lines.

The second set of tests has been performed on more complex scenes, involving sea surface areas, rural regions with distributed targets, as well as urban patterns. An example is shown in Fig. 10. A precise evaluation of the quality of the results obtained is difficult at this point. It can be noticed that the most important targets, as observed in the multilooked image produced by conventional SAR focusing, appear as well in the multilooked image resulting from the imaging technique proposed based on CS, by taking only 50% of the lines. Similarly, features relevant to topography, urban areas, roads, etc., are observable in both images. The closest observation reveals differences between both results in some areas. For example, a high reflective area appears for the recovery by means of CS in the right part of the image, and this does not happen for the image retrieved with a matched filter. This area has been marked with a red circle in the outputs.

A zoom of the large scene in Fig. 10, corresponding to an urban area, is shown in Fig. 11.

V. Conclusion

This paper has suggested a novel approach for radar imaging based on CS. Essentially, it has proposed an alternative to matched filtering for the retrieval of the illuminated scene from the received signal by assuming that the recovered image is sparse or, in wider terms, compressible. After justifying this alternative, the results were analyzed on 1-D simulated sparse data, comparing them to the ones obtained through the conventional matched filter. In this test, on a simulated set of data, the option based on CS is considerably more accurate than that of the matched filtering in terms of amplitude and phase, even if it employs just 50% of the received samples.

Then, an approach has been proposed as an alternative focusing technique to the traditional matched filtering for SAR raw data. The range compression was performed, as usual,

according to an RDA, and then, the azimuth compression was carried out following a CS scheme. The acceptable quality of the images obtained was assessed through qualitative comparison with images obtained with conventional SAR imaging.

The most noticeable advantage of the alternative method presented is the reduction of data to be collected. The option explored in this paper performs the recovery of the illuminated scene through a random selection of the received samples, neglecting the remaining ones. Since the selection of samples is done *a posteriori* and since CS algorithms do not require the Nyquist theorem to be satisfied, we can expect to obtain successful results even with special figures of the selection of samples (for example, with a regular sampling). Nevertheless, from an efficiency point of view, it is not optimum to neglect a fraction of the data acquired. Hence, it would be more interesting to explore different systems of acquisition which would take high profit of the CS theory.

Another advantageous property of the technique proposed is the absence of sidelobes. The tests on simulated data have proven that this fact can improve the accuracy in terms of resolution of the recovered scene (the resolution understood as the capability of the discrimination of close targets). Those tests were carried out on examples entirely satisfying sparsity, which is not always a valid hypothesis in the real world. Therefore, in order to enhance the results obtained on real data with the proposed approach, it would be necessary to define a suitable basis for the compression. Since according to the literature, radar data are compressible, this basis exists.

Further studies explore the extension of the processing on SAR data based on CS both to the range and the azimuth. Moreover, since this solution is not highly dependent on the transmitted waveform, different options of transmitted signal are to be investigated. The transmitted signal can be tuned to improve efficiency or at least to be more suited for a particular application.

ACKNOWLEDGMENT

The authors would like to thank the ESA for providing the SAR image. The authors would also like to thank the anonymous reviewers for their helpful comments.

REFERENCES

[1] U. Benz, K. Strodl, and A. Moreira, "A comparison of several algorithms for SAR raw data compression," *IEEE Trans. Geosci. Remote Sens.*, vol. 33, no. 5, pp. 1266–1276, Sep. 1995.

[2] I. McLeod, I. Cumming, and M. Seymour, "ENVISAT ASAR data reduction: Impact on SAR interferometry," *IEEE Trans. Geosci. Remote Sens.*, vol. 36, no. 2, pp. 589–602, Mar. 1998.

[3] J. E. Nilsson and H. Warston, "Radar with separated subarray antennas," in *Proc. Int. Radar Conf.*, 2003, pp. 194–199.

[4] N. Duffo, I. Corbella, M. Vall-llossera, A. Camps, F. Torres, M. Zapata, J. Benito, and J. Capdevila, "MIRAS imaging validation," in *Proc. IGARSS*, 2003, vol. 2, pp. 1226–1228.

[5] D. Donoho, "Compressed sensing," *IEEE Trans. Inf. Theory*, vol. 52, no. 4, pp. 1289–1306, Apr. 2006.

[6] M. Lustig, D. Donoho, and J. Pauly, "Sparse MRI: The application of compressed sensing for rapid MR imaging," *Magn. Resonance Med.*, vol. 58, no. 6, pp. 1182–1185, Dec. 2007.

[7] M. Sheikh, O. Milenkovic, and R. Baraniuk, "Compressed sensing DNA microarrays," ECE Dept., Rice Univ., Houston, TX, Tech. Rep. TREE 0706, May 2007.

[8] F. Herrmann and G. Hennenfent, "Non-parametric seismic data recovery with curvelet frames," *Geophys. J. Int.*, vol. 173, no. 1, pp. 233–248, Apr. 2008.

[9] R. Willet, M. Gehm, and D. Brady, "Multiscale reconstruction for computational spectral imaging," in *Proc. SPIE Comput. Imaging V, Electron. Imaging*, San Jose, CA, Jan. 2007, p. 649 80L.

[10] S. Cotter and B. Rao, "Sparse channel estimation via matching pursuit with application to equalization," *IEEE Trans. Commun.*, vol. 50, no. 3, pp. 374–377, Mar. 2002.

[11] S. Chen, D. Donoho, and M. Saunders, "Atomic decomposition by basis pursuit," *SIAM J. Sci. Comput.*, vol. 20, no. 1, pp. 33–61, Aug. 1999.

[12] S. Mallat and Z. Zhang, "Matching pursuits with time–frequency dictionaries," *IEEE Trans. Signal Process.*, vol. 41, no. 12, pp. 3397–3415, Dec. 1993.

[13] J. Tropp and A. Gilbert, "Signal recovery from random measurements via orthogonal matching pursuit," *IEEE Trans. Inf. Theory*, vol. 53, no. 12, pp. 4655–4666, Dec. 2007.

[14] D. Donoho and Y. Tsaig, "Extensions of compressed sensing," *IEEE Trans. Signal Process.*, vol. 86, no. 3, pp. 533–548, Mar. 2006.

[15] C. Oliver and S. Quegan, *Understanding Synthetic Aperture Radar Images*. Norwood, MA: Artech House, 1998.

[16] J. C. Curlander and R. N. McDonough, *Synthetic Aperture Radar: Systems and Signal Processing*. New York: Wiley, 1991.

[17] K. Langenberg, M. Brandfass, K. Mayer, and T. Kreutter, "Principles of microwave imaging and inverse scattering," *Adv. Remote Sens.*, vol. 2, pp. 163–186, 1993.

[18] R. Bamler and P. Hartl, "Synthetic aperture radar interferometry," *Inv. Probl.*, vol. 14, no. 4, pp. R1–R54, Aug. 1998.

[19] F. Ulaby and C. Elachi, *Radar Polarimetry for Geoscience Applications*. Norwood, MA: Artech House, 1990.

[20] J. Romberg, "Imaging via compressive sampling," *IEEE Signal Process. Mag.*, vol. 25, no. 2, pp. 14–20, Mar. 2008.

[21] J. W. Owens, M. V. Marcelin, B. R. Hunt, and M. Kleine, "Compression of synthetic aperture radar video phase history data using trellis-coded quantization techniques," *IEEE Trans. Geosci. Remote Sens.*, vol. 37, no. 2, pp. 1080–1085, Mar. 1999.

[22] I. G. Cumming and F. H. Wong, *Digital Processing of Synthetic Aperture Radar Data: Algorithms and Implementation*. Norwood, MA: Artech House, 2005.

[23] E. J. Candes and T. Tao, "Decoding by linear programming," *IEEE Trans. Inf. Theory*, vol. 51, no. 12, pp. 4203–4215, Dec. 2005.

[24] E. J. Candes and T. Tao, "Near-optimal signal recovery from random projections: Universal encoding strategies?" *IEEE Trans. Inf. Theory*, vol. 52, no. 12, pp. 5406–5425, Dec. 2006.

[25] R. Baraniuk and P. Steeghs, "Compressive radar imaging," in *Proc. IEEE Radar Conf.*, Waltham, MA, Apr. 2007, pp. 128–133.

[26] K. Varshney, M. Çetin, J. Fisher, and A. Willsky, "Sparse representation in structured dictionaries with application to synthetic aperture radar," *IEEE Trans. Signal Process.*, vol. 56, no. 8, pp. 3548–3561, Aug. 2008.

[27] S. Bhattacharya, T. Blumensath, B. Mulgrew, and M. Davies, "Fast encoding of synthetic aperture radar raw data using compressed sensing," in *Proc. IEEE Workshop Stat. Signal Process.*, Madison, WI, Aug. 2007, pp. 448–452.

[28] D. Donoho and Y. Tsaig, "Fast solution of Ell-1-norm minimization problems when the solution may be sparse," Dept. Stat., Stanford Univ., Stanford, CA, Tech. Rep. 2006-18, 2006.

Mariví Tello Alonso (S'03) was born in Barcelona, Spain. She received the degree in telecommunication engineering from the Universitat Politècnica de Catalunya (UPC), Barcelona, in 2003. She is currently working toward the Ph.D. degree in multiscale post-processing techniques for the unsupervised interpretation of SAR images in the scope of maritime applications such as vessel monitoring, coastline extraction, and oil-spill detection in the Remote Sensing Laboratory, Signal Theory and Communications Department, UPC, since 2003.

Since January 2010, she also has been with the Institut Català de Ciències del Clima, Barcelona. She is involved in remote-sensing applications related to climate change. Her research interests include fundamental signal processing applied to remote-sensing data.

Paco López-Dekker (S'98–M'03) was born in Nijmegen, The Netherlands, in 1972. He received the Ingeniero degree in telecommunication engineering from the Universitat Politècnica de Catalunya (UPC), Barcelona, Spain, in 1997, the M.S. degree in electrical and computer engineering from the University of California, Irvine, in 1998, under the Balsells Fellowships, and the Ph.D. degree from the University of Massachusetts, Amherst, in 2003, for his research on clear-air imaging radar systems to study the atmospheric boundary layer.

From 1999 to 2003, he was with the Microwave Remote Sensing Laboratory, University of Massachusetts. In 2003, he was with Starlab, which is a privately held company, where he worked on the development of global navigation satellite system-reflection sensors. In 2004, he was a Visiting Professor with the Telecommunications and Systems Engineering Department, Universitat Autonoma de Barcelona. From March 2006 to November 2009, he was with the Remote Sensing Laboratory, UPC, where he conducted research on bistatic synthetic aperture radar (SAR) under a five-year Ramon y Cajal Grant awarded to him in 2005. At the university, he taught courses on signals and systems, signal processing, communications systems and radiation, and guided waves. Since November 2009, he has been the Head of the SAR Missions Group, Microwaves and Radar Institute, German Aerospace Center, Oberpfaffenhofen, Germany. His current research focused on the study of future SAR missions and novel mission concepts.

Jordi J. Mallorquí (S'93–M'96) was born in Tarragona, Spain, in 1966. He received the Ingeniero degree in telecommunications engineering and the Doctor Ingeniero degree in telecommunications engineering for his research on microwave tomography for biomedical applications from the Universitat Politècnica de Catalunya (UPC), Barcelona, Spain, in 1990 and 1995, respectively.

Since 1993, he has been teaching with the School of Telecommunications Engineering of Barcelona, UPC, first as an Assistant Professor and then, since 1997, as an Associate Professor. His teaching activity involves microwaves, radionavigation systems, and remote sensing. For a sabbatical year, he was with the Jet Propulsion Laboratory, Pasadena, CA, in 1999, where he worked on interferometric airborne synthetic aperture radar (SAR) calibration algorithms. His current research interests include working on the application of SAR interferometry to terrain-deformation monitoring with orbital, airborne, and ground data, to vessel detection and classification from SAR images, and to 3-D electromagnetic (EM) simulation of SAR systems. He is also collaborating in the design and construction of a ground-based SAR interferometer for landslide control. Finally, he is currently developing the hardware and software of a bistatic opportunistic SAR for interferometric applications using European Remote Sensing, Envisat, and TerraSAR-X as sensors of opportunity. He has published more than 80 papers on microwave tomography, EM numerical simulation, and SAR processing, interferometry, and differential interferometry in refereed journals and international symposia.